

Selecting representative days for capturing the implications of integrating intermittent renewables in generation expansion planning problems

Kris Poncelet, *Student Member, IEEE*, Hanspeter Höschle, *Student Member, IEEE*, Erik Delarue, *Member, IEEE*, Ana Virag, and William D'haeseleer, *Member, IEEE*,

Abstract—Due to computational restrictions, energy-system optimization models (ESOMs) and generation expansion planning models (GEPMs) frequently represent intra-annual variations in demand and supply by using the data of a limited number of representative historical days. The vast majority of the current approaches to select a representative set of days relies on either simple heuristics or clustering algorithms and comparison of different approaches is restricted to different clustering algorithms. This paper contributes by: (i) proposing criteria and metrics for evaluating representativeness, (ii) providing a novel optimization-based approach to select a representative set of days and (iii) evaluating and comparing the developed approach to multiple approaches available from the literature. The developed optimization-based approach is shown to achieve more accurate results than the approaches available from the literature. As a consequence, by applying this approach to select a representative set of days, the accuracy of ESOMs/GEPMs can be improved without increasing the computational cost. The main disadvantage is that the approach is computationally costly and requires an implementation effort.

Index Terms—Energy-system planning, Generation expansion planning, Power system modeling, Wind energy integration, Power system economics

NOMENCLATURE

A. Abbreviations

<i>CE</i>	Correlation error
<i>DC</i>	Duration curve
<i>ESOM</i>	Energy-system optimization model
<i>GEPM</i>	Generation expansion planning model
<i>IRES</i>	Intermittent renewable energy sources
<i>LP</i>	Linear programming
<i>MILP</i>	Mixed integer linear programming
<i>NRMSE</i>	Normalized root-mean-square error
<i>RDC</i>	Ramp duration curve
<i>REE</i>	Relative energy error
<i>RLDC</i>	Residual load duration curve

B. Sets

\mathcal{B} (index b)	Set of bins
----------------------------	-------------

K. Poncelet, E. Delarue and W. D'haeseleer are with the Department of Mechanical Engineering, KU Leuven and EnergyVille, Belgium. Kris Poncelet holds a PhD grant of the Flemish Institute of Technological Research (VITO)

H. Höschle is with the Department of Electrical Engineering, KU Leuven and EnergyVille, Belgium. H. Höschle holds a PhD grant of the Research Foundation - Flanders (FWO) and the Flemish Institute for Technological Research (VITO).

A. Virag is with the Flemish Institute of Technological Research (VITO) and EnergyVille, Belgium.

\mathcal{C} (index c)	Set of duration curves
\mathcal{D} (index d)	Set of potential representative days
\mathcal{M} (index m)	Set of medium-term periods
\mathcal{P} (index p)	Set of original time series
\mathcal{T} (index t)	Set of time steps

C. Parameters

$A_{c,b,d}$	Share of the time of day d during which the lowest value of the range corresponding to bin b of duration curve c is exceeded
$L_{c,b}$	Share of the time during which the values of a time series with corresponding duration curve c exceed the lowest value of the range corresponding to bin b
N_{repr}	Number of representative periods to select
N_{total}	Total number of repetitions required to scale up the duration of a single representative period to one year

D. Variables

$error_{c,b}$	Error in approximating duration curve c at the bottom of bin b
u_d	Binary selection variable of day d
w_d	Weight assigned to day d , i.e., the number of times the representative period is assumed to be repeated within a single year

I. INTRODUCTION

BOTTOM-UP energy-system optimization models (ESOMs), such as TIMES [1] and MESSAGE [2], and generation expansion planning models (GEPMs), such as LIMES-EU [3] and ReEDS [4] are used frequently to underpin energy policy by performing scenario analyses for the transition of the energy/electricity system. In such models, investment and operational decisions are optimized simultaneously given certain exogenous parameters, e.g., the projected evolution of fossil fuel prices.

Due to the fact that ESOMs and GEPMs typically cover a time horizon of multiple decades, are technology rich and span a large geographical area, solving these models is computationally demanding. To maintain tractability, these models typically use a low level of temporal and geographical detail. However, due to the highly variable, unpredictable

and location-specific characteristics of intermittent renewable energy sources (IRES), such as solar PV panels and wind turbines, using a high level of temporal and geographical detail becomes increasingly important. In this regard, Pfenninger et al. [5] identify resolving details in time and space as the main challenge for this group of models.

Traditionally, large-scale ESOMs represent seasonal and diurnal variations in demand and supply by disaggregating a year into a limited number of so-called time slices (e.g., [4], [6], [7]). For each variable time series (e.g., the load or wind speed), the value assigned to a specific time slice thus corresponds to the average value of that part of the time series corresponding to the specific time slice. While such a stylized representation of the temporal dimension achieves a reasonable accuracy for systems with a low penetration of IRES, several authors have recently shown that for systems with a high penetration of IRES, this approach leads to an underestimation of the variability of IRES, and hence to an overestimation of the potential uptake of IRES, an overestimation of the use of baseload technologies and an underestimation of the value of flexible technologies [8]–[10].

Multiple ways to improve the modeling of the temporal dimension have recently been developed. The current literature mainly focuses on increasing the temporal resolution, i.e., increasing the number of diurnal time slices (e.g., [8], [9]). Nevertheless, it has been shown that increasing the temporal resolution is not sufficient to grasp the inherent variability of IRES [8], [10]. Different approaches to model the temporal dimension to account for the variability of IRES have been analyzed in [10], where it is shown that using the data of a well-chosen set of historical days to represent an entire year can be a suitable approach. However, a justified selection of a representative set of historical periods is not straightforward. Nevertheless, several planning models make use of some sort of representative periods to reduce the computational cost. Well-known examples are a.o. the US-REGEN model developed by the Electric Power Research Institute (EPRI) [11], the POTEnCIA model recently developed by The Institute for Prospective Technological Studies (IPTS) of the European Commission's Joint Research Centre [12] and the LIMES-EU model developed by the Potsdam Institute of Climate Impact Research [3]. Other examples can be found in [13], [14].

The literature contains various approaches to select a representative set of historical periods. Nevertheless, frequently a set of representative days (also referred to as typical days or type-days) is used in planning models without documenting how these days are selected, e.g., [15], [16]. In other work, the set of representative days is obtained by using simple heuristics, e.g., [17]–[20], sometimes supplemented by randomly selecting some additional days, e.g., [14], [21]. As pointed out by de Sisternes [22], a consistent criterion to select these representative periods or to assess the validity of the approximation is lacking. In general, the idea behind most of these simple heuristic approaches is to select a number of periods with different load and/or meteorological conditions in order to capture a variety of different events. As an example, to select three representative days, Belderbos et al. [18] select the day that contains the minimum demand level of the year,

the day that contains the maximum demand level and the day that contains the largest demand spread in 24 hours.

More advanced approaches to select a representative set of historical periods can be divided into two groups. The first and by far the largest group employs clustering algorithms to cluster periods with similar load, wind speed and/or solar irradiance patterns into clusters. For every resulting cluster, either the cluster's centroid or a single historical period from that cluster is taken as the representative period for that cluster. The weight assigned to each representative period, i.e., the number of periods that are represented by this selected period, corresponds to the number of periods that are grouped into its parent cluster. Clustering approaches thus implicitly determine the weight assigned to every selected representative period, which allows to appropriately account for both common and rare events. This is a major advantage compared to the heuristic approaches discussed earlier. To perform the clustering, different algorithms are employed which can be classified into hierarchical and partitional clustering algorithms. A more detailed overview of clustering algorithms is presented in [23]. The goal of all these algorithms is to minimize the sum of the distances between every object (i.e., a period) and the cluster's centroid or median. For the GEPM LIMES-EU, Nahmmacher et al. [24] use Ward's hierarchical clustering algorithm. A similar clustering technique is used in the US-REGEN model to select additional representative periods, after having first used heuristics to select a number of periods containing extreme events [11]. Partitional clustering algorithms, such as k-medoids [23] and k-means [25]–[27] are also frequently used. The performance of the k-means, fuzzy C-means and hierarchical Wards clustering algorithm are evaluated in [23], but the differences between these algorithms were found to be minor for the presented case. Besides clustering algorithms, scenario reduction techniques following a similar philosophy as the clustering approaches, such as the fast-backward method, are also employed to select representative periods, e.g., [28].

A second group of approaches aims to optimize the selection of representative periods with respect to a predetermined, user-defined criterion (external validity indices). In this approach, the selection procedure is directly based on evaluating the full set of representative periods using external validity indices, whereas in the heuristic and clustering approaches, the selection is based on the characteristics of individual historical periods or the "similarity" between individual historical periods; this is a clear fundamental distinction. To the best of our knowledge, the only optimization-based approach in the field of energy research is presented by de Sisternes and Webster [22]. In their approach, the set of weeks which best approximates the residual load duration curve (RLDC) is selected by enumerating all possible combinations of a predetermined number of representative weeks. While this approach is shown to achieve good results, it has a number of limitations. First, the number of combinations for selecting k representative periods out of n candidate periods equals $\frac{n!}{(k!(n-k)!)}$, and thus strongly increases with both the number of candidate periods and the number of periods to select. As a consequence, enumeration is only computationally feasible

for selecting up to 5 weeks out of 52. Therefore, using this approach to optimally select a number of representative days instead of weeks is computationally infeasible. Second, the approach does not determine the optimal weights for each selected period. Finally, the approximation of the RLDC is used as a decision criterion, but the RLDC is dependent on the investments in IRES. Therefore, the approach cannot be used for models with endogenous investments in IRES.

Although multiple approaches to selecting representative periods are available from the literature, there is no consistent comparison of the quality of these different approaches. In this regard, the current literature is restricted to comparing different clustering algorithms. More complete information on the quality of different approaches is vital for ESOMs and GEPMs as a better selection of a representative set of historical periods allows to improve the accuracy of these models without increasing computational complexity.

Moreover, despite the multitude of different approaches to select representative periods, there is not a single optimization-based approach in the field of energy research that can be used to select a sufficiently high number of representative periods.

The aim of this paper is to identify a sound approach for selecting representative historical periods. To this end, (i) criteria and metrics for representativeness are proposed, (ii) a novel optimization-based approach is presented and (iii) this approach is compared to different approaches available in the literature in terms of both accuracy and ease of use.¹

The remainder of this paper is structured as follows. Section II discusses the different temporal aspects which are important to capture in ESOMs and GEPMs, and derives corresponding metrics to evaluate the representativeness of the selected periods. Section III provides an overview of the different approaches considered in this work and presents our novel optimization-based approach. Next, the data and assumptions are presented in Section IV, while the results of the different approaches are discussed in Section V. In Section VI, these different approaches are applied to a test case to illustrate the value of a good selection of representative days. Finally, the main conclusions are presented in Section VII.

II. TEMPORAL ASPECTS

Fig. 1 illustrates the concept of using a representative set of historical periods (e.g., days or weeks) in ESOMs/GEPMs. As is illustrated in this figure, the tool to select a representative set of periods takes different time series as input, for instance quarter-hourly load and wind generation data of multiple years. The output is a representative set of periods and the weights given to each of these representative periods, i.e., the number of times the representative period is assumed to be repeated within a single year. In the ESOM/GEPM, balance of generation (gen) and demand (DEM) is imposed in every time step t (e.g., quarter-hour) of every selected period d . Power generation gen_g by every technology/plant g is restricted by the installed capacity (cap_g). The fixed

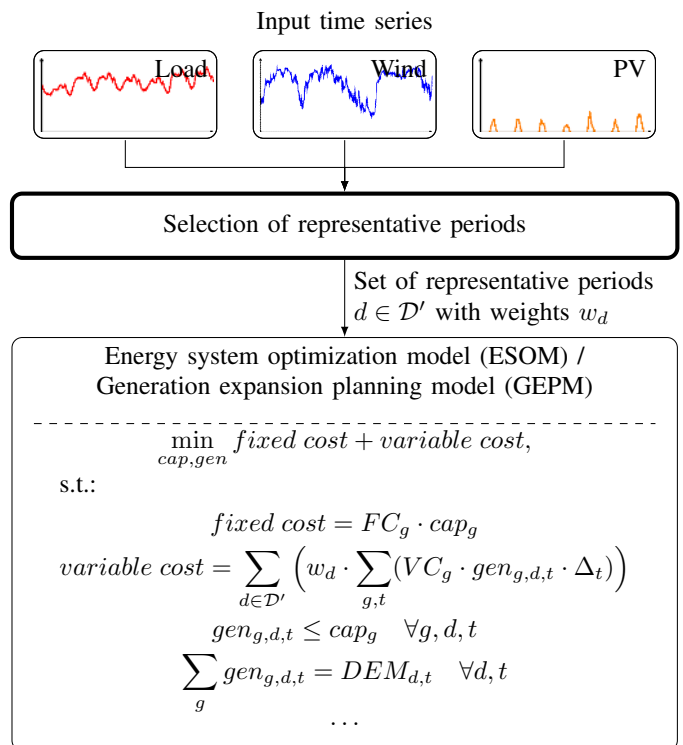


Fig. 1. Schematic of the use of a set of representative historical periods in ESOMs/GEPMs.

costs relate to the construction and fixed operations and maintenance of this capacity. Variable costs, comprising fuel costs, variable operations and maintenance costs and taxes are related to the generation levels of every technology/plant in the selected periods. The weights of each representative period are used to scale the variable costs incurred in the selected periods to an equivalent annual cost. Similarly, fuel consumption and emissions during the selected periods can be scaled to equivalent annual amounts. Thus, the representative set of periods is used to endogenously determine a good approximation of the amount of electricity that is generated by different technologies/units and the associated costs, emissions and fuel use without requiring to optimize the operations over an entire year.

To effectively quantify the accuracy of approximating different time series (e.g., load, wind generation) by a set of representative periods, appropriate metrics must be defined. To this end, the different temporal aspects that impact the results of ESOMs/GEPMs are identified. From the literature [11], [24], [29], we synthesize the following list of temporal aspects:

- 1) the annual load and average IRES capacity factors;
- 2) the distribution of values for each time series
- 3) the correlation between the different time series;
- 4) the variability of each time series.

First, the selected set of periods should preserve the annual electricity demand and the average IRES capacity factors for each model region. To evaluate the quality of the approximation in this respect, the average value (over all considered time series $p \in \mathcal{P}$) of the relative errors in approximating

¹Ease of use comprises the required effort for implementing the approach, the computational cost of executing the approach as well as the flexibility to incorporate user-specific constraints.

the average value of each time series is used as a metric, see Eq. (1). Since for the case presented here, the relative error in the average value of a time series is identical to the relative error of the energy content of a time series, we refer to this metric as the relative energy error (REE_{av}) in the remainder of this text. Note that we use $|\cdot|$ to refer to the absolute value, while $\|\cdot\|$ is used to refer to the cardinality of a set.

Second, a more stringent requirement is that the distribution of load and IRES generation levels, and their respective frequency of occurrence correspond to the one observed in the entire time series. Regarding the time series for IRES generation, it is crucial to account for both periods of very high IRES generation, during which partial curtailment might be required, and periods of near-zero IRES generation, which determine the need for back-up capacity. Moreover, capturing the distribution of IRES generation is required to account for the reduction in operating hours of different types of dispatchable power plants. Thus, by capturing the distribution of each time series, major challenges related to the integration of IRES are accounted for. Therefore, this criterion, which has also been used in [24], [26], is considered to be the most important criterion for evaluating a set of representative periods. The information regarding the distribution of values and their respective frequency of occurrence can be represented by the duration curve (DC) of the time series.² Therefore, the average normalized root-mean-square error (NRMSE) of the approximation of the DC of each time series is used as a second metric, to which we refer as $NRMSE_{av}^{DC}$ (Eq. (2)). The approximation of the duration curve, \widetilde{DC}_p , can be constructed by sorting the data of the selected periods from high to low while correcting for the fraction of a year that each selected period represents. Below, the index $t \in \mathcal{T}$ is used to refer to a specific time step of the original time series (e.g., quarter-hourly or hourly interval).

$$REE_{av} = \frac{\sum_{p \in \mathcal{P}} \left(\left| \frac{\sum_{t \in \mathcal{T}} DC_{p,t} - \sum_{t \in \mathcal{T}} \widetilde{DC}_{p,t}}{\sum_{t \in \mathcal{T}} DC_{p,t}} \right| \right)}{\|\mathcal{P}\|} \quad (1)$$

$$NRMSE_{av} = \frac{\sum_{p \in \mathcal{P}} \left(\frac{\sqrt{\frac{1}{\|\mathcal{T}\|} \cdot \sum_{t \in \mathcal{T}} (DC_{p,t} - \widetilde{DC}_{p,t})^2}}{\max(DC_p) - \min(DC_p)} \right)}{\|\mathcal{P}\|} \quad (2)$$

Third, the correlation between different time series can impact results. Within a single region, this correlation (e.g., between the load and solar PV generation) influences the RLDC, and therefore the expected number of operating hours of different thermal generation technologies. In addition, it impacts the need for curtailment of IRES, as well as their market value [30]. Moreover, the correlation between different regions is important to account for geographical smoothing effects of the load, solar PV generation, and particularly wind generation, and the corresponding value of transmission grids [29]. As a metric to quantify whether the actual correlation is captured by the selected representative periods, the average absolute difference between the correlation based on the data

of the entire time series, and the correlation based on the data in the selected representative periods is used. This is referred to as the average correlation error (CE_{av}) in the remainder of this text (Eq. (3)). The Pearson correlation coefficient is used to quantify the correlation $corr_{p_1, p_2}$ between two time series $p_1, p_2 \in \mathcal{P}$ (Eq. (4)). Here, $V_{p_1, t}$ represents the value of time series p_1 in time step t . Moreover, \bar{V}_{p_1} and \bar{V}_{p_2} indicate the mean value of time series p_1 and p_2 respectively. As the Pearson correlation coefficient has a value of 1 in case of total positive correlation, a value of 0 in case of no correlation and a value of -1 in case of total negative correlation, the values for CE_{av} lie in the range [0,2].

$$CE_{av} = \frac{2}{\|\mathcal{P}\| \cdot (\|\mathcal{P}\| - 1)} \cdot \left(\sum_{p_i \in \mathcal{P}} \sum_{p_j \in \mathcal{P}, j > i} |corr_{p_i, p_j} - \widetilde{corr}_{p_i, p_j}| \right) \quad (3)$$

$$corr_{p_1, p_2} = \frac{\sum_{t \in \mathcal{T}} ((V_{p_1, t} - \bar{V}_{p_1}) \cdot (V_{p_2, t} - \bar{V}_{p_2}))}{\sqrt{\sum_{t \in \mathcal{T}} (V_{p_1, t} - \bar{V}_{p_1})^2 \cdot \sum_{t \in \mathcal{T}} (V_{p_2, t} - \bar{V}_{p_2})^2}} \quad (4)$$

Fourth, the dynamics of fluctuating load and IRES generation time series can impact results. Short-term fluctuations, on time scales of minutes up to hours, are important to account for the limited flexibility of dispatchable power plants (e.g., maximum ramp rates, minimum up and down times), as well as the potential of storage technologies. To quantify to what extent the distribution of short-term fluctuations is captured, we introduce the concept of a ramp duration curve (RDC). The RDC for each time series is found by differentiating and subsequently sorting the original time series. Accordingly, the metric used is the average NRMSE of the approximation of the RDC ($NRMSE_{av}^{RDC}$):

$$NRMSE_{av}^{RDC} = \frac{\sum_{p \in \mathcal{P}} \left(\frac{\sqrt{\frac{1}{\|\mathcal{T}\|} \cdot \sum_{t \in \mathcal{T}} (RDC_{p,t} - \widetilde{RDC}_{p,t})^2}}{\max(RDC_p) - \min(RDC_p)} \right)}{\|\mathcal{P}\|} \quad (5)$$

Medium-term fluctuations, comprising weekly and seasonal fluctuations, are important to account for the limited energy storage capacities of different storage technologies. For example, longer periods of low wind speeds and solar irradiance, during which stored energy might be exhausted, can determine the need for firm back-up capacity. To what extent medium-term fluctuations are captured depends mainly on the input parameters used for selecting representative periods, rather than the used approach in itself. These input parameters are closely related to the temporal structure of the ESOM/GEPM. Examples of such input parameters include the time interval to which the approach for selecting representative periods is applied (e.g., representative periods can be selected for each month, season or year) and the choice of the duration of each individual selected period (e.g., representative hours, days or weeks). As this paper focuses on approaches to select representative periods rather than the temporal structure

²The DC is found by sorting the entire time series from high to low values.

of ESOMs/GEPMS, no metric is introduced for capturing medium-term dynamics.

III. METHODOLOGY

A. General overview

Different approaches to select representative days are evaluated by comparing all four metrics presented in Section II. The results of this evaluation will be shown for an increasing number of representative days (N_{repr}). The following approaches to select representative days are evaluated:

- 1) Heuristics (H);
- 2) Ward's hierarchical clustering algorithm (CA);
- 3) Random selection (RS);
- 4) MILP optimization model (OPT);
- 5) Hybrid approach: random selection followed by optimal weighting (HYB).

The simple heuristics (H) employed in this work are presented in Tab. I. The total number of days selected is presented in the utmost left column. These days are obtained by selecting for every period (indicated in the second column), the days corresponding to the criteria presented in the third to fifth column.

The clustering algorithm (CA) used is Ward's hierarchical clustering algorithm. Some information was provided in Section I, for a full description of the algorithm, we refer to [24].

The third approach is to repeatedly select a random subset of days (RS), and retain from all these subsets the subset which obtained the lowest errors. This approach is closely related to the enumerative approach used to select a set of representative weeks proposed in [22]. However, calculating the error metrics for all possible subsets of days from a single year is computationally infeasible if the cardinality of the subset exceeds 3. Therefore, the number of randomly selected subsets of days is restricted to 50 000.

The fourth approach (OPT) is a newly developed approach that employs a MILP optimization model to identify which days are selected (binary variables) as well as the weight assigned to each day (linear variables). The model formulation is presented in Section III-B.

Finally, another new and novel, hybrid, approach (HYB) that combines features of the RS and the OPT approach is developed. In this approach, a number of random subsets of days are taken and for each subset, the weight given to each day is optimized. The set of weighted days that achieves the lowest errors is retained. Again, 50 000 randomly selected subsets are taken.

B. Optimization model formulation

1) *Basic model:* As discussed in Section II, primarily, the set of representative days should accurately represent the DC of each time series. An optimization model should therefore be capable of selecting a set of representative days (and associated weights), construct the approximation of the DC based on the selected days and corresponding weights, and calculate a metric for the approximation error that can be minimized. Note that the number of steps of the approximated DC depend

TABLE I
OVERVIEW OF THE SIMPLE HEURISTIC USED TO SELECT A NUMBER OF REPRESENTATIVE DAYS.

N_{repr}	Period	Load	Wind	PV
2	Year	Highest peak, lowest valley	-	-
4	Year	Highest peak, lowest valley	Highest and lowest avg. generation	-
8	Summer, Winter	Highest peak, lowest valley	Highest and lowest avg. generation	-
12	Summer, Winter, Intermediate	Highest peak, lowest valley	Highest and lowest avg. generation	-
24	Spring, Summer, Fall, Winter	Highest peak, lowest valley	Highest and lowest avg. generation	Highest and lowest avg. generation

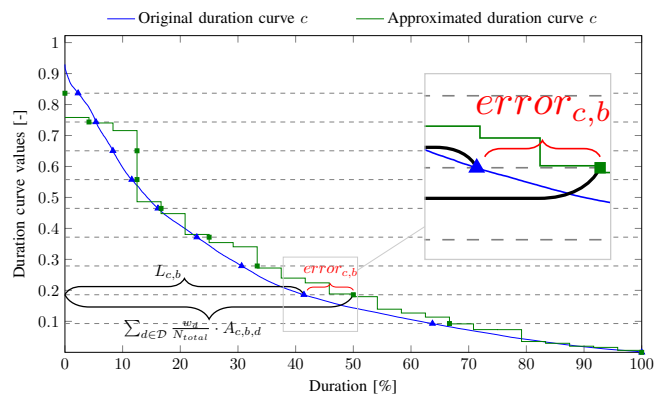


Fig. 2. Visualization of the error term $error_{c,b}$. The duration curve is divided into 10 bins. The error at the bottom of the bin is displayed for bin $b = 8$.

on the number of days selected and the resolution of the data of each day. For example, the approximated DC displayed in Fig. 2 is constructed by selecting 2 representative days with a 2-hourly resolution, resulting in a total of 24 steps. However, obtaining the approximation of the DC requires sorting the values of the selected days which is difficult to integrate in a single optimization framework.

Nevertheless, it is possible to get a clear view on what the approximated DC looks like which does not require sorting the data of the selected days. To this end, each DC $c \in \mathcal{C}$ is divided into a number of bins $b \in \mathcal{B}$, as visualized by the dashed lines in Fig. 2. Each bin thus corresponds to values within a specific range (the highest values belong to the first bin, the lowest values correspond to the last bin). As the original time series is known, the share of time during which this time series has a value greater than or equal to the lowest value in the range corresponding to bin b is known (marked by a \blacktriangle in Fig. 2). For a DC $c \in \mathcal{C}$, this value is represented by the parameter $L_{c,b}$. Similarly, for every potential representative day $d \in \mathcal{D}$, the share of time in day d during which the time series exceeds the lowest value of the range corresponding to a bin b is known. This information is represented by the parameter $A_{c,b,d}$. A graphical representation of this parameter for Belgian load data of 2014 and a number of bins equal to 10 is shown in Fig. 3. This figure shows that, as can be expected, in every day, the

load levels exceed the lowest value of the range corresponding to the last bin in 100% of the time. In contrast, only during a small fraction of the time of some winter days, electricity load values exceed the lower value corresponding to the first bin. This figure also clearly illustrates seasonal and weekly trends.

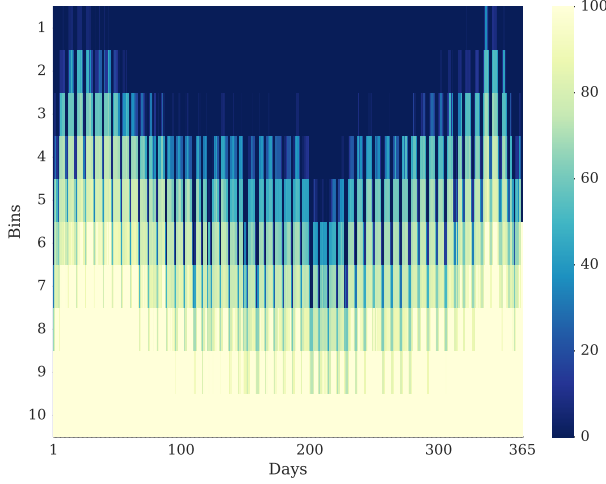


Fig. 3. Graphical representation of the parameter A for the Belgian load during all days of 2014 and a number of bins equal to 10. The color scales indicate the share of time of each day during which the lowest value of the range corresponding to the different bins is exceeded.

Assuming that a subset of representative days $\mathcal{D}' \subset \mathcal{D}$ is selected and a weight w_d is assigned to each selected representative day $d \in \mathcal{D}'$, the share of the time during which the approximated DC has a value greater than or equal to the lowest value in the range corresponding to bin b is also known, i.e., $\sum_{d \in \mathcal{D}'} \frac{w_d}{N_{total}} \cdot A_{c,b,d}$ (indicated by a ■ in Fig. 2). Here, N_{total} reflects the total number of times a single representative period has to be repeated to scale up to an entire year, e.g., N_{total} equals 365 in case representative days are selected and 52 in case representative weeks are selected). Now, if the weight w_d assigned to a day $d \in \mathcal{D}$ can only be non-zero if the day is selected (i.e., $d \in \mathcal{D}'$), the expression can be replaced by $\sum_{d \in \mathcal{D}} \frac{w_d}{N_{total}} \cdot A_{c,b,d}$.

The difference between the original and the approximated DC in the share of the time that the lowest value in the range corresponding to bin b is exceeded is taken as an error metric ($error_{c,b}$). This error term is defined in Eq. (7) and visualized in Fig. 2. Hence, by classifying the data points (e.g., quarter-hourly or hourly values) of all potential representative days into a number of bins, the need to sort the data of the selected days within the optimization in order to obtain a measure for the quality of the approximation is eliminated. The optimization model minimizes the sum of the errors terms, for all considered DCs $c \in \mathcal{C}$ and bins $b \in \mathcal{B}$ by selecting a single set of representative days and corresponding weights, as shown in Eq. (6):

$$\min_{u_d, w_d} \left(\sum_{c \in \mathcal{C}} \sum_{b \in \mathcal{B}} error_{c,b} \right), \quad (6)$$

subject to:

$$error_{c,b} = |L_{c,b} - \sum_{d \in \mathcal{D}} \frac{w_d}{N_{total}} \cdot A_{c,b,d}|, \quad \forall c \in \mathcal{C}, b \in \mathcal{B}, \quad (7)$$

$$\sum_{d \in \mathcal{D}} u_d = N_{repr}, \quad (8)$$

$$w_d \leq u_d \cdot N_{total}, \quad \forall d \in \mathcal{D}, \quad (9)$$

$$\sum_{d \in \mathcal{D}} w_d = N_{total}, \quad (10)$$

$$u_d \in \{0, 1\}, \quad \forall d \in \mathcal{D}; \quad w_d \in \mathbb{R}_0^+, \quad \forall d \in \mathcal{D}. \quad (11)$$

Equation (8) imposes that the number of selected periods corresponds to the predefined number of representative periods N_{repr} . Equation (9) restricts non-zero weights to selected periods, by using a binary variable u_d which indicates whether day d is selected or not. Moreover, the maximum weight that can be assigned to a single selected period is restricted to the number of repetitions required to scale the duration of a single representative period to one year (N_{total}). The weight from all selected periods can therefore be chosen freely, which is important to efficiently account for both common and rare events. Finally, Eq. (10) guarantees that the total duration of the weighted set of representative periods corresponds to one year.

Note that in the HYB approach, the variables u_d are fixed in correspondence to the randomly selected subset, such that only the weights w_d are optimized.

2) *Extended model*: To explicitly account for short-term dynamic aspects in the optimization, the RDC of each time series can be constructed and appended to the set of duration curves $c \in \mathcal{C}$ that need to be approximated. Thus, the model formulation (Eq. (6)-(11)) remains unchanged. The only difference with the basic model is that the set \mathcal{C} not only comprises the DC of each time series, but also the RDC of each time series.

To account for medium-term fluctuations (e.g., seasonal fluctuations), the original time series can be split up into a number of medium-term periods $m \in \mathcal{M}$, where each medium-term period has its own DC. A first option is to select a number $N_{repr,m}$ of representative periods $d \in \mathcal{D}_m$ for each medium-term period individually. Correspondingly, the total weights of the days representative for this medium-term period equals $N_{total,m}$. Thus, the optimization (Eq. (6)-(11)) would have to be repeated $|\mathcal{M}|$ times. An alternative approach would be to add additional constraints to the optimization problem to restrict the approximation error in each medium-term period $m \in \mathcal{M}$.

Up to now, the model does not account for the correlation between different time series. It is important to note from the definition of the sample correlation $corr_{p_1,p_2}$ (Eq. (4)) that both factors in the denominator of the definition of the sample correlation are already approximated implicitly by approximating the DC of time series p_1 and p_2 (as done by the basic model). That is, a set of representative periods which result in a good approximation of the duration curve of a time series p_1 , will also provide a good approximation of $\sum_{t \in \mathcal{T}} (V_{p_1,t} - \bar{V}_{p_1,t})$. However, this does not hold for the numerator of Eq. (4). Therefore, an additional time series

$(V_{p1,t} - \bar{V}_{p1,t}) \cdot (V_{p2,t} - \bar{V}_{p2,t})$ is created. Positive values of this time series correspond to times with a positive correlation, i.e., both $V_{p1,t}$ and $V_{p2,t}$ are either above or below their average value, whereas negative values correspond to times with a negative correlation. Again, a duration curve of this time series can be constructed, and added to the set of duration curves that need to be approximated. The model will then select a set of representative days to not only account for the distribution of each DC, but also to approximate the duration curve of this “correlation duration curve”.

Fig. 4 presents a schematic of the different steps involved in the presented approach.

Unless specifically stated, the results of the OPT and HYB approach, to be presented in Section V, correspond to the basic model, i.e., without extending the model with additional RDCs or time series to improve approximating the correlation.

IV. DATA AND ASSUMPTIONS

A. Data

The original time series used include a time series for the electricity demand, a time series for onshore wind generation and a time series for solar PV generation. All data corresponds to the Belgian electricity system in the year 2014, and is provided by the Belgian transmission system operator on a 15-minute resolution [31]. As one cannot simply assume that the year 2014 is a representative year for the different time series, it is advised to use multiple years of data to construct the different DCs. However, as the goal in this work is to analyze to what extent the different approaches are capable of selecting representative periods to approximate a given original time series, it is reasoned that the size of the original time series will not significantly influence the presented results.

B. Assumptions

The discussion in this work is restricted to selecting days as representative periods as days are more frequently applied than e.g., hours or weeks. For the OPT and HYB approach, a number of bins $\|\mathcal{B}\|$ equal to 40 is used for every DC. Every bin is constructed such that the range of values for each bin is identical. All OPT runs are performed with an optimality gap of 1%, and a maximum solver time of 6 hours. All runs are performed on a Intel®Core™Quad CPU Q9550 @ 2.83GHz×4, with a memory of 13.5GiB, and a 64-bit system.

V. RESULTS

A. Approximation accuracy

The results for all five approaches discussed in Section III-A are presented in Fig. 5-8 and Fig. 10 for the different error metrics. For the approaches based on randomly selecting subsets of representative days (RS and HYB), the distribution of the results of the 50 000 subsets is presented. The box visualizes the median value as well as the 25th and 75th percentiles, whereas the whiskers correspond to the highest and lowest values obtained.

As discussed in Section II, the set of representative days should primarily provide a good approximation of the DC

of each time series. The $NRMSE_{av}^{DC}$ obtained using the different approaches is presented in Fig. 5. As can be seen, the OPT approach obtains the lowest error for all number of days considered. The approximation of the different DCs using the OPT approach to select a varying number of representative days is shown in Fig. 6. The errors obtained using the hybrid approach are only slightly higher (except for selecting 2 representative days, where an identical solution is found). More surprisingly, the errors obtained by approach RS are systematically lower than those obtained using the clustering algorithm even though all days in the RS approach are assigned equal weights. Finally, the errors obtained using the heuristics are high. For all but for two days, more than 75% of the randomly selected sets of days obtains lower errors than those obtained using the heuristics. This is due to the fact that the heuristics aim to account for different types of events, but do not account for their frequency of occurrence.

These results imply that by using a better approach to select a set of representative days, the accuracy of planning models can be improved significantly without increasing the number of time segments (and therefore the computational cost). Seen from a different perspective, this also means that the number of days can be reduced while maintaining a similar accuracy. This can be seen very clearly in Fig. 5, where the OPT and HYB approach using 2 days obtain a similar accuracy as the CA when selecting 8 days. Similarly, the approximation obtained by selecting 4 days using the OPT approach has a similar accuracy than the approximation obtained using the CA to select 24 days.

Fig. 7 displays the REE_{av} for all approaches. For all but the heuristic approach, the average relative energy error is well below 5%. The fact that the heuristics do not properly account for the frequency of occurrence of different events is reflected in the high values for the REE_{av} . As discussed in Section II, approximating the DC of a time series is a more stringent requirement than approximating its average value or energy content. Therefore, sets of days with a low $NRMSE_{av}^{DC}$ also have a low REE_{av} . This can be seen in the inner box plots for the RS and HYB approach, which show the distribution of the REE_{av} for the 1% subsets of days that obtained the lowest $NRMSE_{av}^{DC}$. Fig. 7 displays furthermore that for the RS, OPT and HYB approach, the REE_{av} is very small. Therefore, the differences between these approaches are of less importance, e.g., for 12 days, the REE_{av} equals 0.21%, 0.12% and 0.01% in the RS, OPT and HYB approach respectively.

The error in approximating the correlation between the different time series is shown in Fig. 8. The CE_{av} tends to decline with an increasing number of days. Again, the range of the CE_{av} is high for randomly selected days. However, differently from the REE_{av} , a low $NRMSE_{av}^{DC}$ does not guarantee a low CE_{av} . This can be seen in the inner box plots which show the distribution of the CE_{av} for the 1% subsets of days that obtained the lowest $NRMSE_{av}^{DC}$. As a consequence, if the correlation is not explicitly accounted for in the OPT and HYB approaches, the CE_{av} for these approaches can be relatively high. As discussed in Section III-B2, the correlation can be accounted for in the OPT approach by approximating an additional DC for every pair of time series for which the

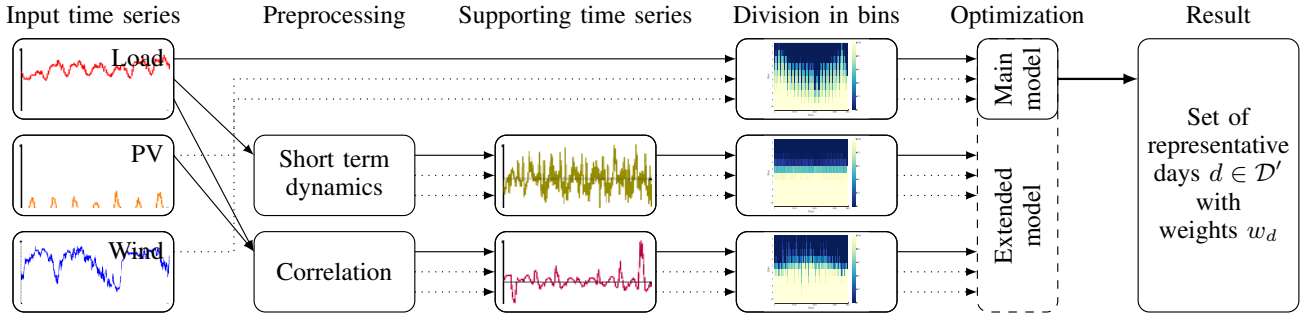


Fig. 4. Schematic of the different steps of the OPT approach.

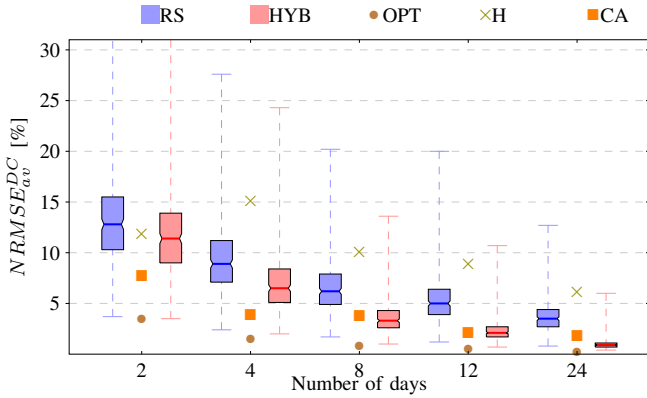


Fig. 5. Error in approximating the DCs.

correlation is important to capture. However, this will lead to a trade-off between the $NRMSE_{av}^{DC}$ and the CE_{av} , as is shown in Fig. 9. This figure illustrates that the CE_{av} obtained with the OPT approach can be greatly reduced with only a minor increase in the $NRMSE_{av}^{DC}$. In contrast, the CA groups together days with similar conditions for all time series and therefore already implicitly accounts to some extent for the correlation between the considered time series. This is reflected in the results shown in Fig. 8 where the CE_{av} for the clustering approach is consistently relatively low.

The errors for approximating the RDCs for all approaches are presented in Fig. 10. A first thing that can be noted is that these errors are significantly lower than for the approximation of the DCs. Moreover, only a moderate decrease of this error with the number of representative days can be observed. Similarly to the CE_{av} , a good approximation of the DCs (low $NRMSE_{av}^{DC}$) does not imply a good approximation of the RDCs (low $NRMSE_{av}^{RDC}$). Nevertheless, there is some correspondence between the $NRMSE_{av}^{DC}$ and the $NRMSE_{av}^{RDC}$. This is because the probability distribution of the ramp of a time series is dependent on the actual value of this time series (e.g., at periods of very high load, it is unlikely that the load will further increase). As a result, sets of days which approximate the DC of each time series with a high accuracy, have a higher probability of capturing the distribution of ramps. To improve capturing the distribution of ramps in the OPT approach, the RDCs can be added to the optimization, as discussed in Section III-B2. This would again lead to a trade-off between approximating the DCs and the RDCs.

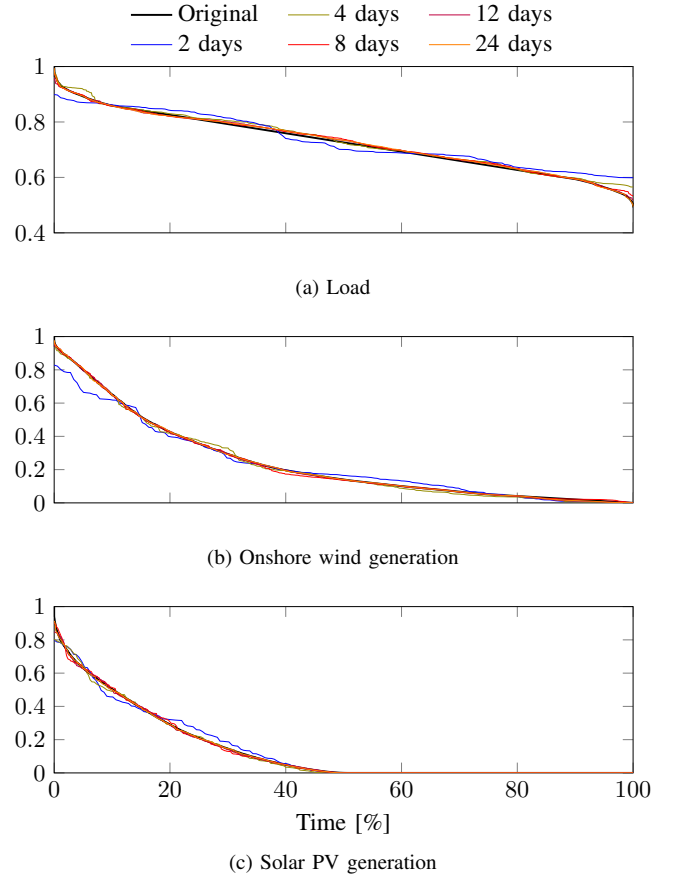


Fig. 6. Approximation of the DCs using the OPT approach to select a varying number of representative days

Following the same reasoning as for the CE_{av} , the clustering approach already implicitly accounts for some dynamics of the considered time series.

Reducing the errors in capturing different temporal aspects for a given number representative periods is particularly important for applications with a high computational cost. For these applications, the OPT and HYB approaches are shown to achieve the best results, closely followed by the RS approach. However, for applications where the computational cost is less stringent, other aspects, such as the effort required for implementing, the computational cost of executing and the flexibility of the approach can be decisive for the approach to use.

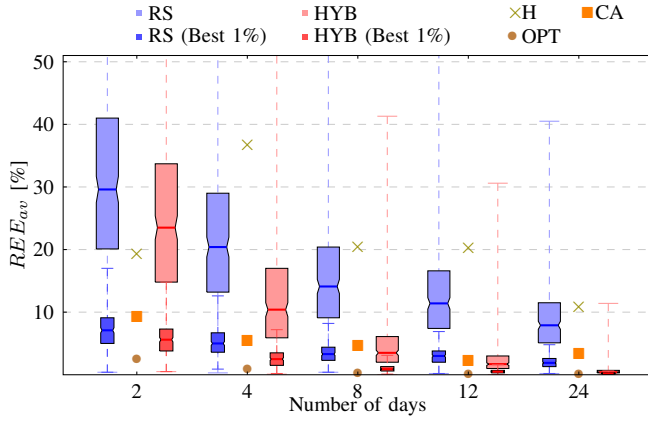


Fig. 7. Error in approximating the average value.

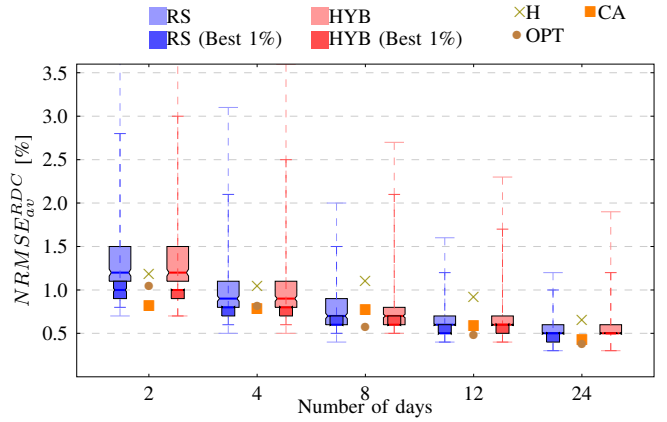


Fig. 10. Error in approximating the RDCs.

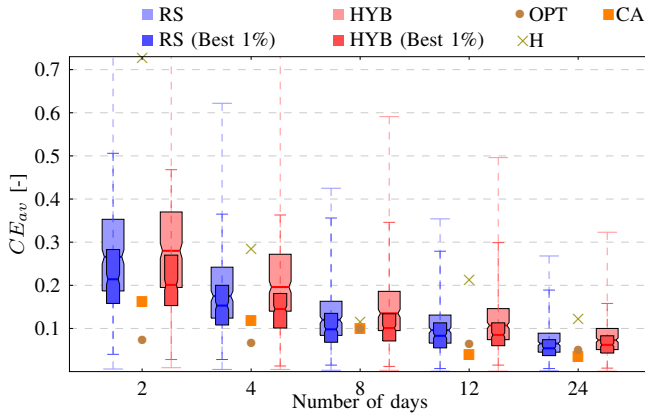


Fig. 8. Error in approximating the correlation.

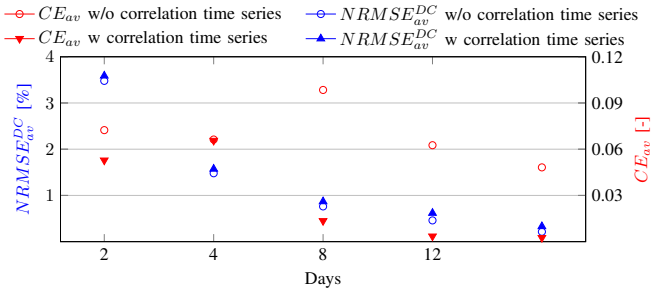


Fig. 9. Impact of including the correlation time series in the OPT approach.

B. Ease of use

In terms of the implementation effort, the H and RS approaches require the lowest effort, while the CA, OPT and HYB approaches all require a more significant implementation effort. In addition, the OPT approach requires the availability of solvers for MILP problems. In an ongoing project funded by the Energy Technology Systems Analysis Program³ (ETSAP), the OPT approach is fine-tuned for direct application in combination with the TIMES model generator. In this regard, the implementation effort of the OPT approach will be eliminated.

The computational resources required to solve the MILP

³ETSAP is an implementing agreement of the International Energy Agency. More information can be found on following website: <http://www.iea-etsap.org/web/index.asp>.

problem used in OPT are high. As mentioned in Section IV-B, a relative optimality gap of 1% is applied but the solver is stopped if no solution satisfying this criterion is found within 6 hours. For all instances except for the case where only 2 representative days were selected, the solver timed out after 6 hours. In contrast, the clustering approach using Ward's hierarchical clustering algorithm can be solved within a few minutes. Finally, both the RS and HYB approach face a high computational cost. Despite the fact that the HYB approach requires solving an additional LP model for every randomly selected subset of days, the computational cost of the RS and HYB approach is similar (as long as the same amount of randomly selected subsets of days are used in both approaches). More specifically, the computation time is on average 1.27 seconds and 1.75 seconds for a single randomly selected set of days in the RS and HYB approach respectively⁴. The difference in time corresponds to the time needed to optimize the weights. Hence, the time required to calculate the error metrics for every subset of days dominates the calculation time. Calculating the error metrics for the 50 000 subsets of days is computationally demanding.

A trade-off between the accuracy of the solution and the number of evaluated subsets of days can be made. This trade-off is visualized in Fig. 11, which again shows the approximation error of the DCs for the different approaches. Suppose only 100 randomly selected subsets of days are used in the RS and HYB approach, the resulting $NRMSE_{av}^{DC}$ (i.e., the lowest $NRMSE_{av}^{DC}$ of these 100 subsets) depends on which 100 subsets are taken. By repeatedly taking 100 random subsets, the distribution of the error obtained for the best subset can be constructed. This cumulative distribution is shown in Fig. 11 for both the RS and HYB approach and both for the case where 100 and 10 000 subsets would be used. A first thing to observe is that, even if the number of subsets is reduced to 10 000 in the RS approach, the accuracy of this approach is higher than for the CA approach with a very high probability. For the HYB approach, this remains valid even

⁴For the results of the paper, the implementation of the RS and HYB approach has been done in python 2.7.11. More advanced programming languages, specified to do bulk computations on large datasets including sorting algorithms, can lower the computation time.

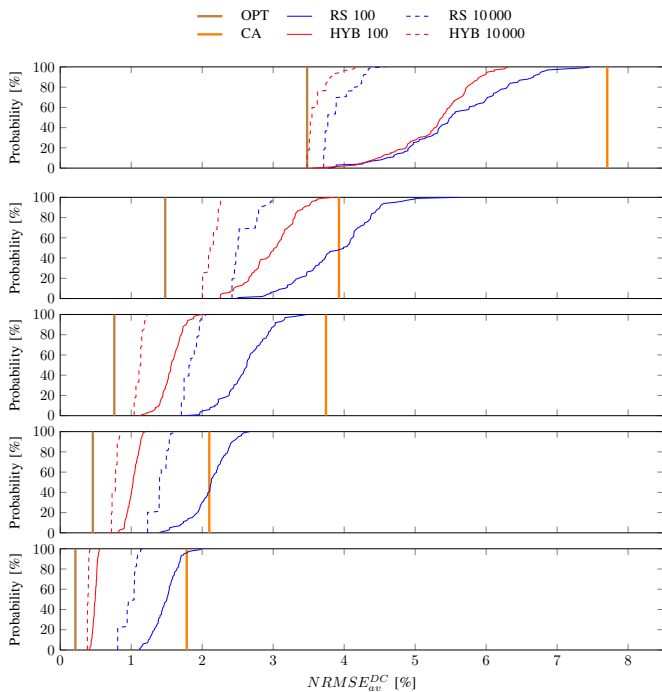


Fig. 11. Error in approximating the DCs. The five panels refer from top to bottom to the results for 2,4,8,12 and 24 representative days.

if the number of subsets would be reduced to 100. Another interesting observation is that, for a low number of days, it is mainly the number of subsets that determines the accuracy of the result. However, as the number of days increases, the value of using a high number of subsets decreases (i.e., the difference between the full and dotted lines decreases). In contrast, the value of optimizing the weights of the randomly selected days (i.e., the difference between the blue and red curves) is relatively low if a low number of days is selected, but increases with the number of representative days. To conclude, the number of subsets of days, and thus the execution cost, can be significantly reduced without a big loss in accuracy if a high number of representative days needs to be selected, and more so in the HYB approach than in the RS approach.

The value of having an approach to more accurately select a set of representative periods depends on the computational restrictions of the ESOM/GEPM. In case there is a hard limit on the computational cost, and hence, the number of representative periods that can be used, the OPT approach allows to improve the accuracy of the ESOM/GEPM. In other cases, the presented approach allows to reduce the computational cost of the ESOM/GEPM by using a smaller number of better selected representative days while achieving the same quality of model outcome in terms of accuracy and representation of power system characteristics. In these cases, it is up to the user to make the trade-off between spending additional computational resources on the approach to select representative periods, or on the ESOM/GEPM. However, it is important to realize that ESOMs/GEPMs are typically used for scenario analysis (and additional sensitivity analyses). As a result, the ESOM/GEPM needs to be solved numerous times. In contrast, the approach to select a representative set of historical periods has to be

executed only once.

Finally, the flexibility to use the approach for different applications is important. A frequently encountered case where the flexibility of the approach is valuable is if the user wants to force certain days into the solution (e.g., the day containing the yearly peak in electricity demand). An efficient implementation of this additional constraint of the problem is straightforward in the RS, OPT and HYB approach, but less so in the CA approach.

To summarize, a qualitative overview of the discussed strengths and weaknesses of the different approaches is presented in Tab. II.

TABLE II
STRENGTHS AND WEAKNESSES OF THE CONSIDERED APPROACHES

Criterion	H	CA	RS	OPT	HYB
Accuracy	--	+-	+	++	++
Implementation cost	++	-	++	--	--
Execution cost	++	+	--	-	-
Flexibility	-	-	+	++	++

VI. TEST CASE

This section presents a test case where the sets of representative days obtained by the different approaches are used in a GEPM. The resulting capacity mix, costs and computation time will be compared to a reference run using the entire time series.

The GEPM used here is the LUSYM (Leuven University SYstem Modeling) investment model. This model aims to minimize the total discounted system cost. This total system cost comprises investment costs, fixed operations and maintenance costs and the costs related to the operation of the power system (consisting of fuel costs, costs related to carbon emissions and start-up costs). For a comprehensive description of the model, we refer to [13]. The GEPM is applied to determine the cost-optimal capacity and generation mix to achieve a 35% share of renewable electricity generation in a power system loosely inspired by the Belgian one. In the presented case, it is assumed that no existing generation capacity is present, i.e., the model is run in a "greenfield" mode. It must be stressed that the case presented here is highly simplified and serves only as an illustration of the use and possible implications of using different approaches to select a set of representative days.

The capacity mix resulting from the run using the entire time series and the runs using 2 representative days selected by the different approaches are presented in Fig. 12. Deviations with respect to the reference case can be observed. For the OPT, RS and CA approach, these differences are relatively minor. In contrast, if the days are selected using the simple heuristics, these differences are very large. Relatively small differences can be observed in the conventional generation mix. It must be noted that, in order to ensure an adequate system, the GEPM has a constraint for the minimum level of dispatchable capacity. The differences in the amount and type of IRES required to meet the renewable energy target

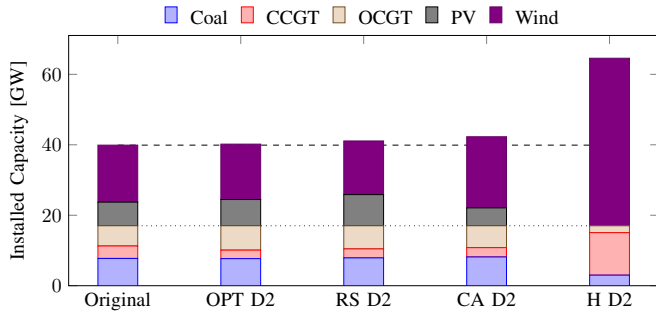


Fig. 12. Installed capacity in the reference run comprising the entire series, and for the runs using 2 representative days selected by the different approaches.

are more pronounced. This is related to how well the sets of days approximate the wind and solar generation time series. As can be seen in Fig. 13, the days selected by the OPT approach provide a relatively good approximation of the wind and solar generation DCs. In contrast, the days selected by the CA and the H approach have significantly higher deviations, particularly for solar PV generation. Both the CA and H approach underestimate solar generation, leading to fewer investments in solar PV generation and a higher dependence on wind turbines to meet the renewable energy target.

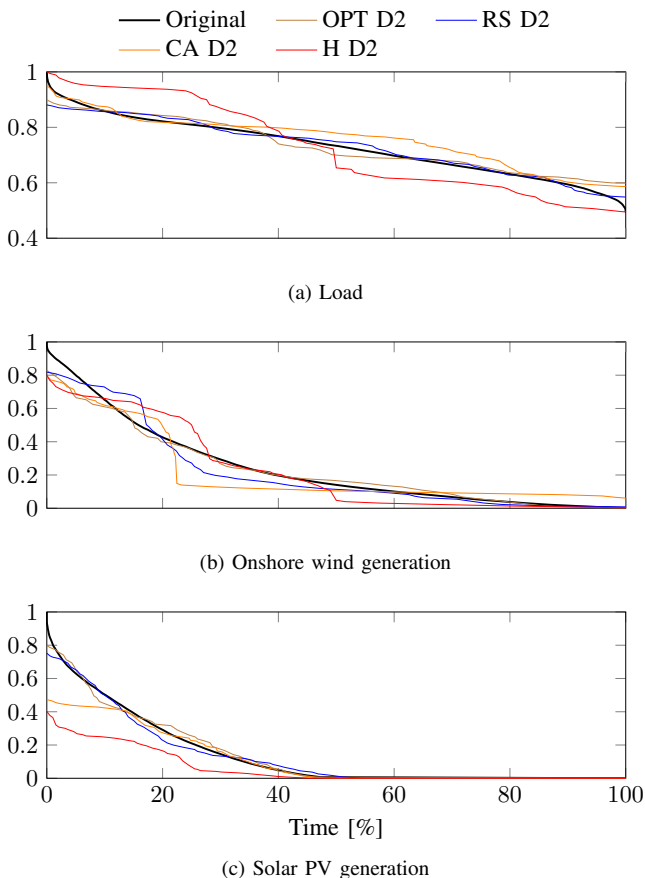


Fig. 13. Approximation of the duration curves for 2 representative days selected by the different approaches.

By using only a limited set of historical days, the GEPM has imperfect information regarding the annual cost related to

operating any given system. Therefore, the GEPM aiming to minimize the total system cost comprising of both investment and operational costs will not be able to find the global optimum. This is reflected in Fig. 12 by the investment decisions deviating from the investment decisions in the reference case. To evaluate this sub-optimality, the cost of operating a system with the capacity mix resulting from each model run is re-evaluated using the entire time series. The projected and re-evaluated total system costs are presented in Table III. The sub-optimality is the difference between the re-evaluated cost and the cost in the reference case, and is presented between brackets as a percentage of the total system cost in the reference case. The results show that by using 2 representative days selected by the OPT approach, this sub-optimality equals a mere 0.29% for the presented case. For the best randomly selected combination of days, this sub-optimality increases to 0.72%, while for the days selected by the clustering algorithm, the deviation increases to 2.57%. Using the simple heuristics, this sub-optimality is significantly higher.

In general, by having a better selected set of days, the model has more accurate information regarding the annual cost of operating any given power system, and is therefore more likely to find a solution close to the global optimum. However, it is important to note that having better information does not necessarily lead to better decision making in every single case. For this reason, the results presented in this test case should not be seen as an attempt to quantify the value that can be added by a better selection of representative days, but rather as an illustration of how the selection of a set of representative days can impact the accuracy of the results and the computation time of ESOMs/GEPMs.

In terms of the computational cost, this increases non-linearly with the number of time steps considered in the GEPM. For the presented test case, the runs using 2, 4 and 8 representative days took on average 2.7, 9.3 and 22.0 seconds respectively. In contrast, the reference case took over 50,000 seconds (almost 14 hours).

TABLE III
OVERVIEW OF THE TOTAL SYSTEM COSTS IN THE DIFFERENT RUNS

Approach	N_{repr}	Projected cost [M€/a]	Re-evaluated cost [M€/a]
Orig.	365	7071	7071
OPT	2	7221	7092 (+0.29%)
RS	2	7043	7122 (+0.72%)
CA	2	7389	7253 (+2.57%)
H	2	10041	9441 (+33.51%)

VII. CONCLUSIONS

To limit the computational complexity of energy-system optimization models (ESOMs), intra-annual variations in demand and supply are typically modeled by using a low number of time segments. Capturing the challenges related to the integration of intermittent renewable energy sources in this low number of time segments is challenging. The recent literature shows that using the data of a limited number of well-chosen representative historical periods is an approach

that allows doing so without having to drastically increase the number of time segments. In generation expansion planning models (GEPs), the level of temporal detail is typically somewhat higher than in ESOMs. Nevertheless, these models also face computational restrictions which could be alleviated by using a small, but representative set of historical periods. For these reasons, numerous well-known and state-of-the-art ESOMs/GEPs do already make use of a set of representative historical periods to represent variations in demand and supply.

To select a representative set of historical periods, multiple approaches are described in the literature. However, the literature regarding the comparison of different approaches is restricted to comparing different clustering algorithms. Moreover, there is not a single optimization-based approach available in the literature that can be employed to select a large set of representative periods.

In this paper, a new and novel optimization-based approach relying on mixed integer linear programming (MILP) and a derived hybrid approach are presented. The results of these approaches are compared to different approaches available in the literature. Different temporal aspects which can impact the results of ESOMs/GEPs were identified and appropriate metrics were proposed to assess how well these aspects are represented by a set of representative periods.

The novel optimization-based approach and the derived hybrid approach are shown to obtain more accurate results than the approaches available in the current literature. The significance is that by applying the novel approaches to select a set of representative periods, the accuracy of ESOMs/GEPs can be increased without increasing the computational cost. This is illustrated in a simplified test case aiming to determine the cost-optimal capacity mix to obtain a target share of renewable electricity generation in a system inspired by the Belgian power system.

While the focus in this work is on selecting a set of representative days for application in ESOMs/GEPs, the developed approach can be applied to various applications. In addition, as the developed approaches rely on MILP or LP, they are highly flexible to incorporate user-specific constraints. However, the developed approaches also have the disadvantage that solving these approaches themselves can be computationally costly and require some implementation effort.

REFERENCES

- [1] R. Loulou, U. Remne, A. Kanudia, A. Lehtila, and G. Goldstein, *Documentation for the TIMES model: Part I*, ETSAP, April 2005.
- [2] L. Schrattenholzer, "The energy supply model MESSAGE," IIASA Research Report, Tech. Rep., 1981. [Online]. Available: http://www.iiasa.ac.at/publication/more_RR-81-031.php
- [3] P. Nahmmacher, E. Schmid, and B. Knopf, "Documentation of LIMES-EU - a long-term electricity system model for Europe," Potsdam Institute for Climate Impact Research, Tech. Rep., 2014. [Online]. Available: http://www.nrel.gov/analysis/reeds/pdfs/reeds_documentation.pdf
- [4] W. Short et al., "Regional energy deployment system (ReEDS)," NREL Technical Report, Tech. Rep., 2011. [Online]. Available: http://www.nrel.gov/analysis/reeds/pdfs/reeds_documentation.pdf
- [5] S. Pfenninger, A. Hawkes, and J. Keirstead, "Energy systems modeling for twenty-first century energy challenges," *Renewable and Sustainable Energy Reviews*, vol. 33, pp. 74–86, May 2014.
- [6] S. Simoes et al., "The JRC-EU-TIMES model - Assessing the long-term role of the SET Plan Energy technologies," JRC's Institute for Energy and Transport, Tech. Rep., 2013.
- [7] D. Pozo, E. Sauma, and J. Contreras, "A three-level static milp model for generation and transmission expansion planning," *Power Systems, IEEE Transactions on*, vol. 28, no. 1, pp. 202–210, Feb 2013.
- [8] S. Ludig, M. Haller, E. Schmid, and N. Bauer, "Fluctuating renewables in a long-term climate change mitigation strategy," *Energy*, vol. 36, no. 11, pp. 6674–6685, Nov. 2011.
- [9] G. Haydt, V. Leal, A. Pina, and C. A. Silva, "The relevance of the energy resource dynamics in the mid/long-term energy planning models," *Renewable Energy*, vol. 36, no. 11, pp. 3068 – 3074, 2011.
- [10] K. Poncelet, E. Delarue, D. Six, J. Duerinck, and W. D'haeseleer, "Impact of the level of temporal and operational detail in energy-system planning models," *Applied Energy*, vol. 162, pp. 631–643, Jan. 2016.
- [11] D. Young et al., "Program on technology innovation: US-REGEN model documentation 2014," EPRI, CA: 2014. 3002004693, Tech. Rep., 2014. [Online]. Available: <http://www.epri.com/abstracts/Pages/ProductAbstract.aspx?ProductId=00000003002004693>
- [12] L. Mantzos et al., "POTEnCIA model description - version 0.9," European Commission, Joint Research Centre Institute for Prospective Technological Studies, Tech. Rep., 2016. [Online]. Available: <http://publications.jrc.ec.europa.eu/repository/handle/JRC100638>
- [13] A. van Stiphout, K. De Vos, and G. Deconinck, "The impact of operating reserves on investment planning of renewable power systems," *Accepted for publication in IEEE Transactions on Power Systems*, May 2016.
- [14] M. Fripp, "Switch: A Planning Tool for Power Systems with Large Shares of Intermittent Renewable Energy," *Environmental Science & Technology*, vol. 46, no. 11, pp. 6371–6378, Jun. 2012.
- [15] M. Fürsch et al., S. Hagspiel, C. Jägemann, S. Nagl, D. Lindenberger, and E. Tröster, "The role of grid extensions in a cost-efficient transformation of the European electricity system until 2050," *Applied Energy*, vol. 104, pp. 642 – 652, 2013.
- [16] D. J. Swider and C. Weber, "The costs of wind's intermittency in Germany: application of a stochastic electricity market model," *European Transactions on Electrical Power*, vol. 17, no. 2, pp. 151–172, Mar. 2007.
- [17] C. Yuan, C. Gu, F. Li, B. Kuri, and R. Dunn, "New problem formulation of emission constrained generation mix," *Power Systems, IEEE Transactions on*, vol. 28, no. 4, pp. 4064–4071, Nov 2013.
- [18] A. Belderbos and E. Delarue, "Accounting for flexibility in power system planning with renewables," *International Journal of Electrical Power & Energy Systems*, vol. 71, pp. 33–41, Oct. 2015.
- [19] M. Haller, S. Ludig, and N. Bauer, "Decarbonization scenarios for the EU and MENA power system: Considering spatial distribution and short term dynamics of renewable generation," *Energy Policy*, vol. 47, pp. 282–290, Aug. 2012.
- [20] D. S. Kirschen, J. Ma, V. Silva, and R. Belhomme, "Optimizing the flexibility of a portfolio of generating plants to deal with wind generation," in *2011 IEEE PES General Meeting*, Jul. 2011, pp. 1–7.
- [21] E. K. Hart and M. Z. Jacobson, "A Monte Carlo approach to generator portfolio planning and carbon emissions assessments of systems with large penetrations of variable renewables," *Renewable Energy*, vol. 36, no. 8, pp. 2278–2286, Aug. 2011.
- [22] F. J. de Sisternes and M. D. Webster, "Optimal Selection of Sample Weeks for Approximating the Net Load in Generation Planning Problems," Jan. 2013. [Online]. Available: <http://citeseerx.ist.psu.edu/viewdoc/download?doi=10.1.1.362.8358&rep=rep1&type=pdf>
- [23] M. S. ElNozahy, M. M. A. Salama, and R. Seethapathy, "A probabilistic load modelling approach using clustering algorithms," in *2013 IEEE PES General Meeting*, Jul. 2013, pp. 1–5.
- [24] P. Nahmmacher, E. Schmid, L. Hirth, and B. Knopf, "Carpe Diem: A Novel Approach to Select Representative Days for Long-Term Power System Models with High Shares of Renewable Energy Sources," [Online]. Available: <http://dx.doi.org/10.2139/ssrn.2537072>
- [25] S. Fazlollahi, S. L. Bungener, P. Mandel, G. Becker, and F. Marchal, "Multi-objectives, multi-period optimization of district energy systems: I. Selection of typical operating periods," *Computers & Chemical Engineering*, vol. 65, pp. 54–66, Jun. 2014.
- [26] W. Omran, M. Kazerani, and M. Salama, "A clustering-based method for quantifying the effects of large on-grid pv systems," *Power Delivery, IEEE Transactions on*, vol. 25, no. 4, pp. 2617–2625, Oct 2010.
- [27] M. Nick, R. Cherkaoui, and M. Paolone, "Optimal allocation of dispersed energy storage systems in active distribution networks for energy balance and grid support," *Power Systems, IEEE Transactions on*, vol. 29, no. 5, pp. 2300–2310, Sep 2014.
- [28] S. Jin, A. Botterud, and S. Ryan, "Temporal versus stochastic granularity in thermal generation capacity planning with wind power," *Power Systems, IEEE Transactions on*, vol. 29, no. 5, pp. 2033–2041, Sept 2014.

- [29] C. Golling, "A cost-efficient expansion of renewable energy sources in the European electricity system: an integrated modelling approach with a particular emphasis on diurnal and seasonal patterns," Ph.D. dissertation, University of Cologne, 2012. [Online]. Available: <http://kups.ub.uni-koeln.de/id/eprint/4856>
- [30] L. Hirth and F. Ueckerdt, "The Decreasing Market Value of Variable Renewables: Integration Options and Deadlocks," in *Transition to Renewable Energy Systems*. Wiley-VCH Verlag GmbH & Co. KGaA, Jun. 2013, pp. 75–92.
- [31] ELIA, "Grid data - Elia," Apr. 2015. [Online]. Available: <http://www.elia.be/en/grid-data>



William D'haeseleer received a M.S. in electro-mechanical engineering in 1980 and a M.S. in nuclear engineering in 1982, both from the KU Leuven, Belgium, and a M.S. in electrical engineering in 1983 and the Ph.D. degree in 1988, both from the University of Wisconsin-Madison, Madison, WI, USA. Currently, he is a full-time Professor at the KU Leuven and Director of the KU Leuven Energy Institute



Kris Poncelet received a M.S. in mechanical engineering in 2013 from the University of Leuven (KU Leuven), Belgium. Since 2013, he has been working as a Ph.D. researcher at the KU Leuven on energy-system and power-system planning. The research of Kris Poncelet is supported by a Ph.D. grant provided by the Flemish Institute for Technological Research (VITO).



Hanspeter Höschle received the Diplom degree in industrial engineering and management in 2012 from the Karlsruhe Institute of Technology, Germany. Since 2012, he has been working as a Ph.D. researcher at the KU Leuven, Belgium, on power system economics and the modeling of electricity markets, in particular capacity remuneration mechanisms. He holds a Ph.D. fellowship of the Research Foundation - Flanders (FWO) and the Flemish Institute for Technological Research (VITO).



Erik Delarue received a M.S. in mechanical engineering in 2005 and the Ph.D. degree in mechanical engineering in 2009, both from the KU Leuven, Belgium. Currently, he is an Assistant Professor and research fellow of the Research Foundation Flanders (FWO) at the KU Leuven.



Ana Virag received a M.S. in electrical engineering from the University of Zagreb. After that, she has been conducting her Ph.D. research at the Technical University of Eindhoven on identification and control methods for balancing electrical power systems. Since 2015, she joined VITO/EnergyVille where she is working on modelling different energy market mechanisms and on integration of RES and flexibility into the system.